Camelopardalids (IAU#451) from comet 209P/LINEAR

Peter Jenniskens[1]

Since shortly after the comet's discovery in 2004, the close encounter of comet 209P/LINEAR with Earth on 2014 May 29 was highly anticipated as an opportunity to measure past activity of the comet. Only five days earlier, Earth would encounter ejecta from the 18th, 19th and 20th centuries. The outburst was observed from 7–8 km altitude during a SETI Institute sponsored airborne observing campaign. 21 Camelopardalids were detected, for an equivalent peak ZHR $\sim 13 \pm 4$ /h. The meteors were faint, with high magnitude distribution index $\chi = 3.7 \pm 0.5$ in the -1 to $+5$ magnitude range, which translates to a differential mass distribution index of $s = 2.42 \pm 0.15$ (0.003–4 g) and a differential size distribution index of $\alpha = 5.3 \pm 0.4$ (0.2–2 cm). The meteors fragmented excessively towards the end of their trajectory. Twenty trajectories were triangulated in ground-based observations, showing a compact geocentric radiant at RA = $119\overset{\circ}{.}9 \pm 5\overset{\circ}{.}3$, Dec = $+78\overset{\circ}{.}2 \pm 0\overset{\circ}{.}9$, with speed $V_g = 14.9 \pm 0.7$ km/s, close to the predicted position. Light curves were U-shaped, with peak luminosity at 88 km altitude, where a wake faded in 1.08 ± 0.17s (1/e). Activity was of relatively long duration (5-h FWHM). It remains unclear when this dust was ejected.

Received 2014 June 11

1 Introduction

Comet 209P/LINEAR is a weakly active Jupiter Family comet with an orbital period of 5.02 years. Discovered in 2004, it approached Earth to only 0.0554 AU on 2014 May 29, now the 9th closest encounter of a comet to Earth on record and the closest since comet IRAS-Araki-Alcock in 1983. 2014 was the first year the comet orbit evolved to passing close to Earth's orbit, and it will keep doing so until the return of 2044. Other such weakly active comets had past disruptions that created some of our most significant meteor showers, including the alpha Capricornids, kappa Cygnids, Quadrantids and Geminids (Jenniskens, 2008).

Shortly after its discovery, Esko Lyytinen and I realized that, just five days earlier, Earth would pass close to some 19th and 20th century dust trails, assuming that the comet was active in the past (Table 6j of Jenniskens, 2006). Vaubaillon (2012) confirmed that many of the 18th, 19th and early 20th century dust trails would be in Earth's path on 2014 May 24 around 07^h UT, and piled up in a narrow region of nodes. Ye & Wiegert (2014) examined the comet activity in 2009 and concluded that the shower would be broader than predicted by Vaubaillon (2012), peaking slightly earlier, and dominated by bright meteors (particles larger than 1 mm in size, or visual magnitude $M_v < +5.4$ magnitude).

The new meteor shower would be mainly visible from the United States and southern parts of Canada. The expected level of activity was unknown, if any, because there were no prior encounters with the dust ejected by comet 209P/LINEAR. If the comet was not active in the past, there would be no new shower at all. Assuming the activity was the same as today, both Vaubaillon (2012) and Ye & Wiegert (2014) put the expected peak rate within a factor of two from ZHR = 200/h.

[1]SETI Institute, 189 N. Bernardo Ave., Suite 100, Mountain View, CA 94043, USA. Email: petrus.m.jenniskens@nasa.gov

IMO bibcode WGN-423-jenniskens-camelopardalids
NASA-ADS bibcode 2014JIMO...42...98J

The hope that some activity would be observed increased when a weak shower was detected in early May CAMS and SonotaCo video observations (Rudawska & Jenniskens, 2014). The period of activity was later extended to cover the time of the expected outburst (Šegon et al., 2014). This shower was called the Camelopardalids (IAU#451, CAM). That weak activity implied the comet was active in the past, but it remained unknown if that was during the timeframe relevant for the May 24 encounter.

The upcoming activity in 2014, if any, would provide insight into the comet's activity in the centuries before its discovery. Because of the potential that significant dust might be released in the past, the shower was highly anticipated (Jenniskens & Lyytinen, 2014; Rao, 2014).

2 Observing Campaign

California was well positioned for viewing the anticipated shower. If the shower would indeed be skewed towards brighter meteors, then this would not be an easy radar target and flux measurements were best made by optical cameras from the air. The large surface area near the horizon, combined with low extinction, would result in a higher rate of meteors per square degree at the low 5–10° elevations (Gural & Jenniskens, 2000).

The SETI Institute board of trustees chartered a Beechcraft King Air 90 aircraft out of Palo Alto airport to take a team of researchers to 6–8 km altitude for best viewing of the shower. With only 36 hours of advance notice that the mission would proceed, we used the event to practice the rapid response to a possible future announced asteroid impact. Because of that, a mission patch with no date was designed (Figure 1) and team member Ron Dantowitz of Dexter Southfield Schools flew out to California from Brookline, Massachusetts. Local team members included Mike Koop, Jim Albers and Alan Dunton.

Five intensified cameras were deployed in the main cabin, three Gen II of type XX1332 and two of type MX-9916/UV, all providing a star limiting magnitude of +6.9 and a field of view of about $40° \times 30°$, aimed

Figure 1 – The SETI Institute airborne observing campaign to study the new shower from 209P/LINEAR. From left to right: Ron Dantowitz, Peter Jenniskens, Mike Koop and Jim Albers. Right: flight path out of Palo Alto, California. For more information, see the mission website at `http://meteor.seti.org`.

at $\sim 16°$ elevation (Gural & Jenniskens, 2000). During the flight, we performed real-time flux measurements by viewing three of the cameras, a fourth person (Alan) making notes of the count every minute. Results were posted shortly after the flight results were announced the next morning. In addition, Ron fielded two Lumenera 2-1R Silicon based CCD cameras for imaging (resulting in 72 764 spatial images) and spectroscopy (5 200 spectroscopic images).

The mission was supported by ground-based low-light level video observations. Weather permitting, the 60-videocamera CAMS network in the San Francisco Bay Area would measure trajectories, light curves, and pre-atmospheric orbits, and also obtain meteor spectra from the station in Sunnyvale (Jenniskens et al., 2011). In addition, six single-CAMS cameras operated in Brentwood, Walnut Creek, San Mateo College, and Foresthill (administered by Dave Samuels). In the BeNeLux, a 30-camera single-CAMS network was in operation (administered by Carl Johannink), which covered the early and late parts of the meteor shower profile. On the Mid-Atlantic East Coast, Pete Gural administered a 7-camera single-CAMS network and operated one intensified camera at Mt. Airy, MD, of the same type (XX1332, 50mm $f/1.2$ lens) as deployed airborne, set up with $39° \times 49°$ field of view (5.3 arcmin/pixel) pointed to elevation 56° and azimuth 246°.

3 Results

The airborne observations.

Quite to my relief, the shower did show. The wheels left the runway right on time at $05^{h}30^{m}$ UT. In the next half hour, the aircraft climbed to altitude and away from city light and haze. Observations with the cameras viewing west towards the ocean were started at $06^{h}00^{m}$ UT. Eastwards looking cameras were initially hampered by city lights and recorded data starting at

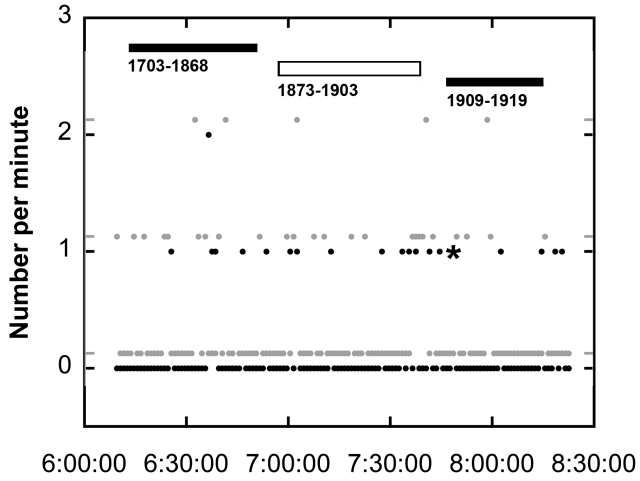

Figure 2 – Count per minute of Camelopardalids from altitude, with sporadic count in gray and offset. Trails: Vaubaillon (2012).

$06^{h}17^{m}$ UT. The aircraft followed a flight path towards the shower radiant (Figure 1). At $07^{h}22^{m}$–24^{m} UT, the aircraft reached the furthest point and turned back to Palo Alto. The sky was mostly clear above the wing tip throughout the flight, but occasionally clouds traversed the 5–10° elevation band. Observations were made until $08^{h}23^{m}$ UT, with the eastward looking cameras becoming much brighter from city lights after $08^{h}18^{m}$ UT.

The observing period covered the full range of encounter times of dust trails calculated by Vaubaillon (2012), who found that the older 17th and early 18th century dust trails tended to be encountered around $06^{h}30^{m}$ UT, while the more recent 1909–1914 trails were expected to peak around $08^{h}00^{m}$ UT (Figure 2).

The occurrence of Camelopardalids is marked in Figure 2. The rate increased gradually during the night, and peaked when crossing the relatively recent 1903 dust trail. The first magnitude +5 Camelopardalid was seen at $06^{h}25^{m}42^{s}$ UT, moving at a $\sim 20°$ angle to the

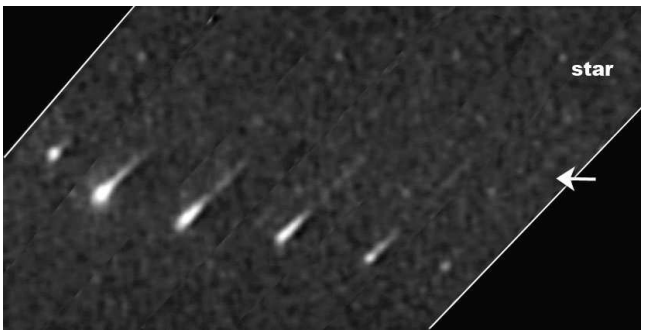

Figure 3 – The 2014 May 24, $07^h48^m12^s.5$–$14^s.9$ UT Camelopardalid in Corvus (compilation of frames at $07^h48^m12^s.5$, $13^s.0$, $13^s.5$, $13^s.7$, $14^s.0$, and $14^s.9$). The arrow points towards the persistent emission.

horizon from the North, gliding through the air with low angular velocity. All video tapes were later viewed again and meteors plotted on gnomonic star charts to confirm radiant association and determine the meteor magnitude relative to the background stars. A total of 21 Camelopardalids and 38 other meteors were detected in the two hours of observations.

Few meteors appeared as low as 5–10°. The star limiting magnitude was good near the horizon, based on counts in area #23 in Corvus. At 11 km altitude, the nominal extinction is less than 0.1 magnitude at 10° elevation and 0.3 magnitude at 5° elevation, about six times lower than on the ground (Gural & Jenniskens, 2000). The fact that we were flying at only 6–8 km did not affect the conditions much. Distant clouds were a problem in some cameras, but a clear stretch from 07^h24^m to 07^h54^m UT in the westward looking cameras only produced one low Camelopardalid, also the brightest of the night (Figure 3). We carefully examined for slow moving meteors, but found no other in the 5–10° band.

The only explanation is that the magnitude distribution index (χ) of the stream was rather high, contrary to expectations. Indeed, most Camelopardalids captured on video had a low apparent visual magnitude. From +5 down brighter magnitudes, we captured: 7, 10, 1, 1, 1, and 1 Camelopardalid, respectively. In contrast, we captured: 6, 10, 13, 2, and 2 for all other meteors. After correction for camera detection efficiency, the calculated $\chi \sim 3.8 \pm 0.8$.

The bright +0.2 magnitude Camelopardalid at $07^h48^m13^s$ UT was distinctly elongated towards the end (Figure 3) and left a persistent emission at peak brightness (altitude $\sim$ 88 km based on triangulated meteors, see below). This emission is orange in color in video by Prof. Peter C. Slansky of the Munich Academy of Television and Film (see front cover), from which the derived 1/e decay time is 1.08 ± 0.17 s (during 3.4 s). The elongation of the meteoroid and an abrupt velocity change past peak brightness (Figure 3) is due to a flare-less whole-scale breakup event into small particles with high surface-to-mass ratio. Dust collection efforts in the upper atmosphere are ongoing, in the hope that this debris may stand out from the normal meteoric influx, taking many days or weeks to settle.

Ground-based observations.

CAMS station operators Jim Albers (Sunnyvale) and Bryant Grigsby (Lick Observatory) quickly made raw data available to be able to confirm the shower radiant. The first Camelopardalid meteor was captured by the CAMS network in the night before the peak, at 04^h48^m UT on May 23. Later that day, CAMS@BeNeLux network administrator Carl Johannink reported that this network captured three more. Most meteors were detected on May 24 by the California network, including one at $06^h41^m13^s$ UT by the SingleCAMS camera stations 216 (Brentwood), 214 (Forrest Hill) and 218 (Walnut Creek), administered by Dave Samuels (Figure 3). Sadly, intermittent clouds hampered observations in California right around the peak between 05^h12^m and 09^h00^m UT. Fourteen trajectories were measured before and after the peak. No spectra were obtained. The CAMS@Mid-Atlantic network had clear weather with magnitude +5.8 skies and administrator Peter Gural calculated one Camelopardalid trajectory. Later that day, the CAMS@BeNeLux network captured one final late Camelopardalid at 22^h27^m UT.

Table 1 summarizes the results of the 20 trajectories, including some that were not so precisely measured and would normally be rejected. Twelve cluster tightly around geocentric radiant RA = $119^\circ.9 \pm 5^\circ.3$, Dec = $+78^\circ.2 \pm 0^\circ.9$, with speed V_g = 14.9 ± 0.7 km/s. The predicted radiant position from dust of comet 209P/LINEAR was RA = 125°, Dec = +78°, with speed $V_g = 15.8$ km/s (Jenniskens, 2006), in good agreement.

Figure 4 shows the distribution of radiant positions measured by all CAMS networks on May 23–24. The Camelopardalids (CAM) stand out well from other shower activity (including the eta Aquariids (#31), the Scorpiid-Sagittariid Complex (#163), chi Librids (#275), and zeta Puppids (#300)) and from the apex and antihelion sporadic sources.

Ten Camelopardalids showed an U-shaped light curve, with a hint of an end flare due to the abundant fragmentation ('A' and 'C' in Figure 5). Peak brightness occurred at around 88 km altitude, near the upper range of other meteors with 19 km/s entry speed (Figure 5). A total of 13 out of 20 meteors (65%) have a light curve peaking early ($F < 0.50$, Table 1), which has been interpreted as typical for fragile meteoroids (Murray et al., 2000). One late bright Camelopardalid showed a more gradual rise ('D'), indicative of a more sturdy meteoroid (Figure 5).

Ten meteor lightcurves were more sharply peaked (V-shape), with peak brightness lower in the atmosphere ('B' and cross in Figure 5). These short tracks produced poor trajectory solutions, as a result of which many have outlaying radiant positions. Ignoring these in Figure 4 (gray symbols) leaves only radiant positions at the compact radiant. It is not clear whether the low altitudes are a physical phenomenon of the meteors, or a problem in the trajectory solution. Other 19 km/s showers also have such solutions in CAMS data.

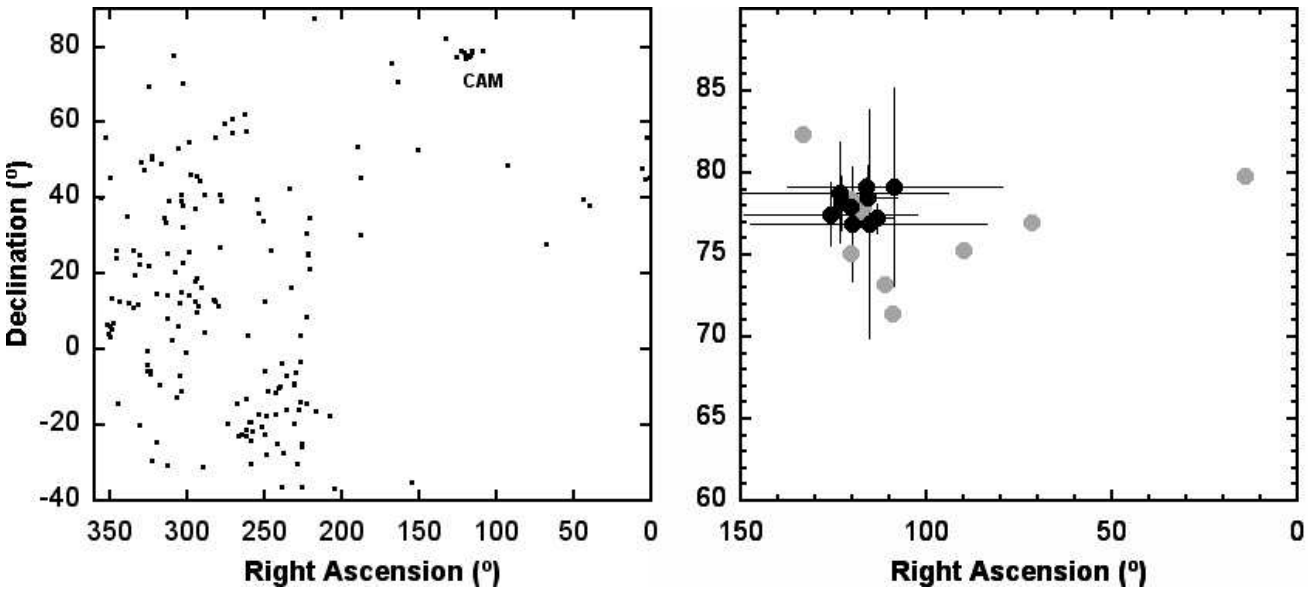

Figure 4 – CAMS-measured geocentric radiant positions on 2014 May 23 and 24. Gray: Meteors with short V-shaped lightcurves.

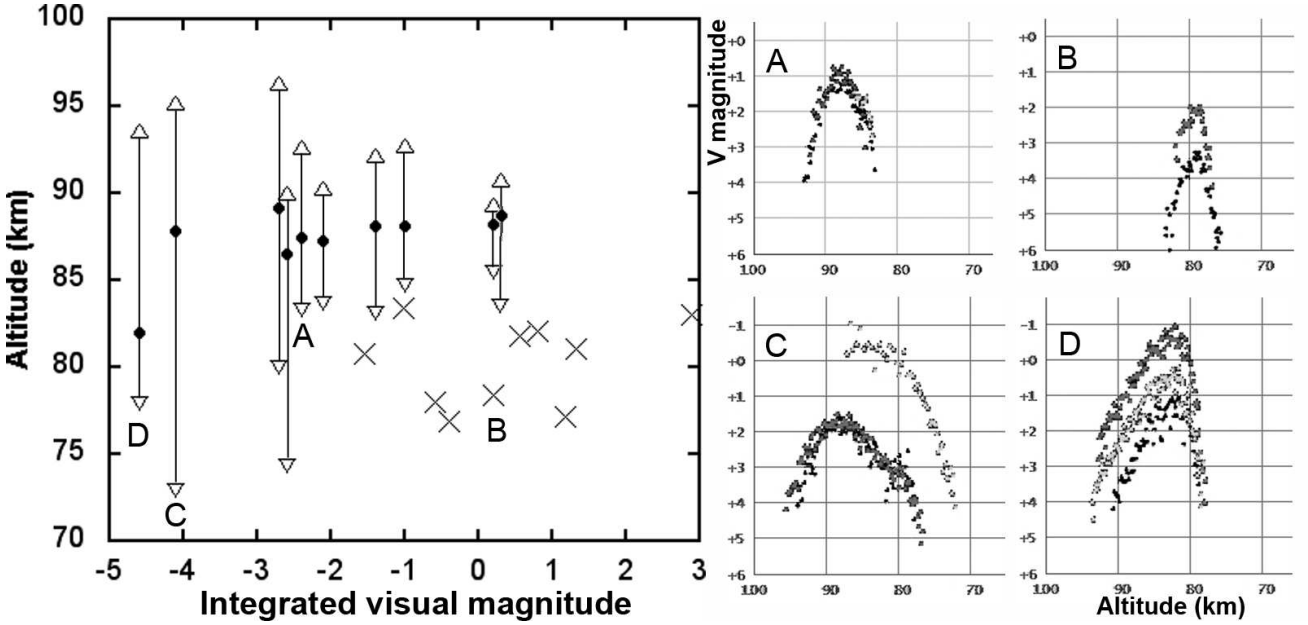

Figure 5 – Example meteor lightcurves and altitude range (• and × mark peak brightness) plotted as a function of the integrated meteor brightness. A: Typical case at $04^{h}41^{m}02^{s}$ UT; B: Likely incorrect, sharply peaked result at $05^{h}15^{m}59^{s}$ UT; C: Single-CAMS result at $06^{h}41^{m}13^{s}$ UT; D: Large meteoroid at $11^{h}34^{m}14^{s}$ UT.

Many of the multi-station Camelopardalids are relatively bright, peaking at +1 and +2 magnitude, but that is an effect of the detection probability of the network. Based on all non-shower (sporadic) meteors triangulated until 2013 March, we have detection probabilities from magnitude +5 down brighter magnitudes: 4e-5, 0.0018, 0.018, 0.080, 0.27, 0.64, 0.98, 1.00, 1.00,... and sporadic $\chi_s = 3.24$. Based on this correction, the Camelopardalids had $\chi = 3.8 \pm 0.4$.

The ground-based intensified camera operated by Pete Gural from a location in Mt. Airy in Maryland, captured 25 Camelopardalids in the 6-h period from $02^{h}00^{m}$ to $08^{h}00^{m}$ UT. The final ten minutes were affected by dew on the lens. The meteors were extracted using Meteor Scan and a new single-track radiant-association algorithm was used to confirm the shower association based on direction and angular velocity. The apparent magnitude distribution from +5 down brighter magnitudes: 11, 10, 4, 0, from which the magnitude distribution index $\chi \sim 3.2$. Nine more single station Camelopardalids were captured in the CAMS@Mid-Atlantic network, all of +3 ($N = 5$) and +4 magnitude. Because the meteors were so faint, the range loss was significant enough for these meteors not to be detected at the other sites, resulting in few two-station coincident observations for triangulation.

Because of clouds, meteor rates are difficult to evaluate from the ground-based CAMS data in California. From the airborne Camelopardalids observed above 15° elevation, we have an equivalent ZHR = 9.9 ± 3.7 at

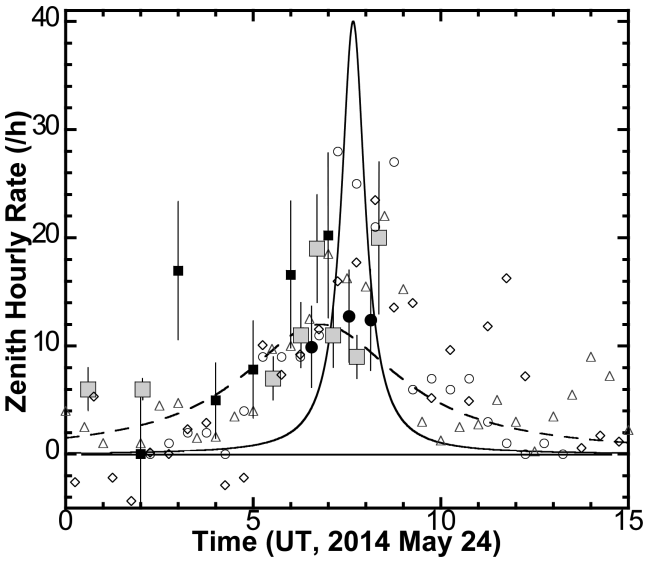

Figure 6 – Activity curve. • = airborne video; ■ = ground-based intensified video; ■ = IMO visual (International Meteor Organization, 2014); open symbols are Radio forward meteor scatter data by Hirofumi Sugimoto (Japan, ○), and scaled to match: Jeff Brower (British Columbia, ◇), and Peter Bus (△). Predictions are those by Vaubaillon (solid line) and Ye & Wiegert (dashed line).

06^h33^m UT, 12.8 ± 4.3 at 07^h33^m UT, and 12.4 ± 4.7 at 08^h08^m UT, but systematic errors may be higher than the random errors. These rates are shown as solid circles in Figure 6. The Mid-Atlantic CAMS stations were clear. The rate of Camelopardalids observed by the Mt. Airy camera translates into the equivalent ZHR values shown as black squares in Figure 6.

The results are compared to radio forward-meteor-scatter counts provided by Jeff Brower of British Columbia and Peter Bus of the Netherlands (Bus, 2014), which were scaled to match the rates from video data. Independently calibrated are similar data published online by Hirofumi Sugimoto from Japan (○), and the IMO calculated near-real time ZHR values (International Meteor Organization, 2014) from visual observations of the shower (open squares, data as of June 9). The graph also shows the predictions by Vaubaillon (2012) as a solid line and by Ye & Wiegert (2014) as a dashed line, both with rates scaled to match the observed profile, a factor 20 less than predicted.

4 Discussion

There is no doubt that we encountered the dust of comet 209P/LINEAR. All prediction models correctly calculated the general time of when this dust was encountered. This is the first meteor outburst observed from ejecta of comet 209P/LINEAR.

That said, it is not so clear to me when this dust was ejected. The steep magnitude distribution index is very interesting, because it means that large particles were lost by processes other than collisions (Jenniskens, 2006). Ye & Wiegert (2014) correctly predicted the 5-h duration of the shower, but perhaps not based on the correct physics of dust ejection. They assumed a dust differential size distribution index $\alpha = 2.6$, based on the large-grain size distribution of dust ejected by 1P/Halley. A relatively long section of the dust trails was integrated, when plotting up the dust density at Earth. Moreover, the dynamics of dust delivery does not reflect their result that particles arriving at Earth would be skewed strongly to larger particles and be mostly larger than 1 mm ($M_v < +5.4$), and the resulting shower dominated by bright meteors. This would suggest a collisionally relaxed $\chi \sim 1.85$ (Jenniskens, 2006).

The observed $\chi = 3.7 \pm 0.5$ translates to a differential mass distribution index $s = 2.42 \pm 0.15$ and size index $\alpha = 5.3 \pm 0.4$. The abundance of faint meteors resulted in an unexpected strong detection by the CMOR radar, which is sensitive predominantly to the brightest underdense echoes of +6 and +7 magnitude (Brown, 2014).

Such a high magnitude distribution index is not unusual. It was also a feature of past Draconid outbursts from hyperactive comet 21P/Giacobini-Zinner ejecta in 1933 ($\chi = 3.6$) and 1946 ($\chi = 3.2$; Jenniskens, 2006). In that case, I suspect that the steep distribution comes from particle ejection being driven by CO_2 outgassing, so that the grains still contained water ice. When that water ice evaporated, the larger grains might have fallen apart into smaller grains. CO_2-driven outgassing would be hard to understand for a weakly active comet like 209P/LINEAR, but ice-laden material could be released in a fragmentation event of the comet itself. Could the 2014 Camelopardalids be an echo of a comet disintegration event in the past? While that is not impossible, the observed 20 times weaker-than-expected rates even from the current weak activity may argue against this.

It is perhaps more likely that the comet was weakly active also in the 18th, 19th, and early 20th centuries. In that case, the steep distribution index could come from the meteoroids falling apart over time. Past crossings of old Leonid dust trails also seemed to show such lower-than-expected peak activity (Jenniskens, 2006). The observed activity is centered on the most recent dust trails according to the times calculated by Vaubaillon (2012). Perhaps, these fragile cometary grains disappear over time by falling apart into finer dust due to thermal or centrifugal stresses. If so, the fading is rapid, with a 1/e timescale of only 30–50 years, assuming an initial dust density equivalent to ZHR = 100–400 in 2014. Are we seeing the accumulated effect of many centuries of fragile cometary meteoroids fading into memory? This should be modeled to see if it can explain the broader than expected shower in the model by Vaubaillon (2003).

Or are simply the particle ejection conditions different than assumed? Were the ejected particles small to begin with? Could ejection conditions have put the small particles preferentially in Earth's path, instead of the large particles? These questions may be answered soon. The comet itself was well observed in this encounter and will provide more insight into the conditions of the present day dust ejection.

Date 2014	Time (UT)	$\lambda_\odot$ (°)	$RA_\infty^\dagger$ (°)	Dec_∞ (°)	V_∞ (km/s)	a_1 (km)	a_2 (/s)	H_b (km)	H_e (km)	M_v (mag)	ΣM_v (mag)	m (g)	F	††	Q (°)	ΔT (s)	Source CAMS
5/23	$04^h48^m17^s$	61.810	143.49	+74.15	17.39	0.00	0.17	84.7	78.1	+1.4	−1.6	0.3	0.63	V	33	0.52	C
			±0.14	±0.66	±0.25	±0.06	±0.08										
5/23	$21^h34^m44^s$	62.482	155.42	+82.55	21.74	1.12	1.12	86.5	77.7	+2.0	+0.7	0.03	0.78	V/U	5	0.55	(B)
			±0.62	±0.82	±0.73	±0.13	±0.16										
5/23	$23^h55^m58^s$	62.576	142.93	+82.42	16.85	0.04	0.17	81.4	76.8	+2.4	+1.2	0.02	0.33	V	66	0.36	B
			±0.59	±0.42	±0.22	±0.05	±0.10										
5/23	$23^h58^m18^s$	62.578	139.71	+81.89	18.80	0.31	0.03	91.2	83.2	+2.7	+0.2	0.05	0.28	U	13	0.56	B
			±0.13	±0.42	±0.88	±0.17	±1.56										
5/24	$04^h11^m21^s$	62.747	142.12	+77.06	18.14	0.02	0.20	92.2	83.1	+2.3	−1.4	0.2	0.45	U	19	0.69	C
			±0.44	±0.30	±0.15	±0.01	±0.15										
5/24	$04^h41^m02^s$	62.766	147.82	+77.49	19.08	0.03	4.75	92.6	83.3	+0.8	−2.4	0.5	0.54	U, fr	30	0.72	C
			±0.11	±0.32	±0.70	±0.02	±0.16										
5/24	$04^h41^m04^s$	62.766	145.16	+78.10	18.30	0.02	0.17	96.3	80.0	+0.2	−2.7	0.7	0.43	U, fr	30	1.25	C
			±0.12	±0.10	±0.10	±0.02	±0.07										
5/24	$05^h15^m59^s$	62.790	137.32	+83.37	14.28	0.00	0.01	83.5	82.0	+0.8	−1.0	0.15	0.11	V	15	0.15	(C)
			±0.78	±1.07	±0.29	±0.01	±0.10										
5/24	$05^h21^m27^s$	62.793	144.26	+79.46	17.77	0.25	0.55	92.7	84.7	+1.5	−1.0	0.15	0.57	U, fr	38	0.67	C
			±0.15	±0.13	±0.80	±0.08	±0.91										
5/24	$05^h45^m48^s$	62.810	277.21	+86.70	14.87	0.72	2.27	78.2	75.9	+1.4	−0.4	0.08	0.57	V	13	0.30	(C)
			±2.86	±3.18	±1.24	±0.15	±0.35										
5/24	$06^h41^m14^s$	62.847	151.29	+78.63	19.41	0.01	3.77	95.2	72.9	−0.4	−4.1	2.5	0.33	U, fr	10	2.09	sC
			±0.19	±0.66	±0.79	±0.25	±1.60										
5/24	$07^h43^m00^s$	62.888	129.91	+84.26	17.84	0.00*	0.00*	82.4	78.2	+3.7	+1.3	0.02	0.49	V	89	0.42	(M)
			±0.25	±0.28	±0.20	–.–	–.–										
5/24	$07^h51^m41^s$	62.894	151.99	+81.73	16.92	0.00*	0.00*	82.9	75.5	+2.0	−1.1	0.05	0.61	V, fr	27	0.72	C
			±0.16	±0.11	±0.05	–.–	–.–										
5/24	$08^h11^m43^s$	62.907	134.95	+78.56	16.37	0.00	6.39	90.3	83.7	+1.3	−2.1	0.4	0.45	U	42	0.75	(C)
			±7.45	±3.87	±3.64	±0.00	±2.23										
5/24	$08^h37^m07^s$	62.924	148.99	+82.30	18.79	0.01	3.12	90.0	74.3	+1.4	−2.7	0.7	0.36	wd, U	9	1.58	C
			±0.03	±0.12	±0.06	±0.00	±0.02										
5/24	$09^h25^m53^s$	62.957	144.44	+83.14	15.27	0.00	0.18	82.1	80.2	+2.1	+0.8	0.03	0.01	V	32	0.23	(C)
			±2.75	±2.15	±0.80	±0.05	±0.41										
5/24	$09^h37^m39^s$	62.964	280.25	+87.35	12.94	0.00	0.01	83.3	81.7	+4.4	+2.9	0.004	0.17	V	23	0.19	(C)
			±2.53	±1.34	±0.69	±0.01	±0.29										
5/24	$10^h01^m17^s$	62.980	128.86	+83.55	18.81	0.03	0.54	89.3	85.5	+1.9	+0.2	0.05	0.29	U	20	0.39	(C)
			±0.85	±1.38	±0.08	±0.03	±0.10										
5/24	$11^h34^m15^s$	63.042	119.17	+84.91	18.89	0.00	0.00*	93.7	77.9	−0.9	−4.6	4.0	0.73	sl, U	19	1.56	C
			±0.12	±0.07	±0.03	–.–	–.–										
5/24	$22^h27^m23^s$	63.478	162.34	+79.99	14.09	0.00	0.08	86.3	81.2	+2.7	+0.5	0.04	0.27	V	63	0.44	B
			±0.34	±0.28	±0.13	±0.02	±0.10										

Table 1 – Trajectory and lightcurve data of Camelopardalids from CAMS data. The a_1 and a_2 are parameters that describe the deceleration (Jenniskens et al., 2011); H_b, H_e are the beginning and end height of the meteor; M_v is the visual magnitude; ΣM_v is the integrated brightness, expressed in magnitude; m is the mass in grams; F is the relative position of the peak in the light curve (0 = begin, 1 = end); Q is the highest convergence angle of fitted planes to get the first trajectory solution; ΔT is the duration of the meteor. The source abbreviations are: C = CAMS network in California; sC = product of participating single CAMS stations; B = CAMS@BeNeLux; M = CAMS@MidAtlantic. A letter between brackets means that the measurement does not meet the normal CAMS precision criteria.

† Errors in Right Ascension are given as $\Delta RA \cos(Dec)$. a_1 and a_2 are defined in Jenniskens et al. (2011).

†† Notes: U = U-shaped; V = flare, V-shaped; fr = fragmentation (end flare), wd = wide; sl = slow rise.

Table 1 – (Continued)

Date 2014	Time (UT)	$\lambda_\odot$ (°)	RA_g (°)	Dec_g (°)	V_g (km/s)	q (AU)	$1/a$ (1/AU)	a (°)	i (°)	ω (°)	Ω (°)	Π (°)
5/23	$04^h48^m17^s$	61.810	120.3	+75.1	13.5	0.969	0.440	2.27	17.2	152.0	61.807	213.8
			±2.6	±0.8	±0.4	±0.006	±0.036		±0.4	±2.4	±0.002	±2.4
5/23	$21^h34^m44^s$	62.482	133.3	+82.4	18.7	0.970	0.222	4.50	24.9	154.8	62.478	217.3
			±12.6	±4.3	±0.9	±0.024	±0.127		±1.7	±7.5	±0.002	±7.5
5/23	$23^h55^m58^s$	62.576	117.1	+77.9	12.7	0.968	0.524	1.91	17.2	150.1	62.578	212.6
			±5.5	±4.6	±0.3	±0.007	±0.069		±1.3	±3.6	±0.001	±3.6
5/23	$23^h58^m18^s$	62.578	120.6	+78.4	15.2	0.966	0.387	2.58	20.0	151.8	62.578	214.4
			±7.6	±8.6	±1.2	±0.029	±0.081		±2.2	±12.0	±0.003	±12.1
5/24	$04^h11^m21^s$	62.747	115.9	+78.4	14.4	0.964	0.443	2.26	19.2	150.3	62.743	213.0
			±2.6	±2.1	±0.2	±0.005	±0.039		±0.7	±1.9	±0.001	±1.9
5/24	$04^h41^m02^s$	62.766	123.3	+78.8	15.6	0.968	0.368	2.72	20.5	152.4	62.762	215.2
			±9.5	±3.1	±0.8	±0.030	±0.112		±1.3	±10.1	±0.003	±10.1
5/24	$04^h41^m04^s$	62.766	116.5	+79.1	14.6	0.965	0.439	2.28	19.6	150.5	62.763	213.3
			±1.2	±0.6	±0.1	±0.002	±0.015		±0.2	±0.9	±0.001	±0.9
5/24	$05^h15^m59^s$	62.790	71.7	+77.0	9.1	0.943	0.781	1.28	13.2	132.2	62.791	195.0
			±8.8	±4.2	±0.5	±0.025	±0.073		±1.2	±12.5	±0.002	±12.5
5/24	$05^h21^m27^s$	62.793	108.7	+79.1	14.0	0.961	0.491	2.04	19.0	148.3	62.791	211.1
			±9.4	±6.0	±1.1	±0.030	±0.115		±1.8	±10.7	±0.003	±10.7
5/24	$05^h45^m48^s$	62.810	14.4	+79.8	9.8	0.930	0.857	1.17	16.3	121.1	62.809	183.9
			±30.0	±47.9	±2.1	±0.191	±0.290		±7.4	±70.4	±0.054	±70.4
5/24	$06^h41^m14^s$	62.847	125.8	+77.5	16.0	0.968	0.320	3.13	20.6	153.3	62.844	216.1
			±7.6	±2.0	±1.0	±0.026	±0.085		±1.1	±7.5	±0.003	±7.5
5/24	$07^h43^m00^s$	62.888	119.9	+76.9	14.0	0.967	0.441	2.27	18.3	151.2	62.890	214.1
			±1.0	±3.5	±0.3	±0.002	±0.045		±1.1	±0.9	±0.001	±0.9
5/24	$07^h51^m41^s$	62.894	113.2	+77.2	12.8	0.964	0.521	1.92	17.2	148.9	62.894	211.8
			±1.3	±0.9	±0.1	±0.002	±0.017		±0.2	±1.1	±0.001	±1.1
5/24	$08^h11^m43^s$	62.907	109.2	+71.4	12.1	0.958	0.515	1.94	14.9	147.2	62.910	210.1
			±27.9	±51.0	±5.6	±0.162	±0.454		±8.9	±68.9	±12.454	±72.1
5/24	$08^h37^m07^s$	62.924	120.5	+77.9	15.2	0.966	0.383	2.61	19.9	151.6	62.924	214.6
			±0.6	±0.4	±0.1	±0.001	±0.006		±0.2	±0.4	±0.001	±0.4
5/24	$09^h25^m53^s$	62.957	111.5	+73.2	10.5	0.966	0.605	1.65	13.7	147.3	62.962	210.3
			±23.5	±23.2	±1.1	±0.114	±0.248		±5.1	±41.1	±0.175	±41.2
5/24	$09^h37^m39^s$	62.964	89.8	+75.3	6.6	0.963	0.824	1.21	9.5	135.7	62.977	198.6
			±29.7	±54.3	±1.6	±0.173	±0.213		±4.7	±75.1	±5.632	±75.6
5/24	$10^h01^m17^s$	62.980	115.6	+76.9	15.2	0.961	0.381	2.62	19.6	150.4	62.981	213.3
			±10.4	±7.0	±0.1	±0.005	±0.112		±2.3	±2.5	±0.001	±2.5
5/24	$11^h34^m15^s$	63.042	122.8	+78.2	15.3	0.967	0.379	2.64	20.1	152.2	63.043	215.2
			±0.3	±1.6	±0.1	±0.001	±0.022		±0.5	±0.2	±0.001	±0.2
5/24	$22^h27^m23^s$	63.478	117.7	+77.2	8.7	0.975	0.710	1.41	12.4	147.4	63.484	210.9
			±3.5	±1.9	±0.2	±0.006	±0.025		±0.4	±3.4	±0.001	±3.4
209P/LINEAR		65.694	120.6	+73.9	15.8	0.904	0.341	2.932	19.35	150.3	65.691	216.0

Acknowledgements

I thank the SETI Institute board of trustees and CEO David Black for their sponsoring of the aircraft deployment and support of the public outreach effort. Diane Gilbert and Dave Samuels operated cameras that streamed video live to the internet. Esko Lyytinen did the original prediction calculations. CAMS@Benelux station-operators Steve Rau, Klaas Jobse, Martin Breukers, Robert Haas, Felix Bettonvil, Erwin van Ballegoij, Piet Neels and Carl Johannink contributed to this work. Peter Gural developed single-track association algorithms for this work. Jeff Brower, Peter Bus, and Ilkka Yrjola of Global-MS-Net contributed radio forward meteor scatter observations. CAMS is supported by the NASA Planetary Astronomy and NASA Near Earth Object Observation programs.

References

Brown P. (2014). "Camelopardalid meteors". *Central Bureau Electronic Telegrams*, **3886**.

Bus P. (2014). "Radiowaarnemingen van de uitbarsting van de mei camelopardaliden". *eRadiant*. (June 2014 issue, in Dutch).

Gural P. S. and Jenniskens P. (2000). "Leonid storm flux analysis from one Leonid MAC video AL50R". *Earth, Moon and Planets*, **82-83**, 221–247.

International Meteor Organization (2014). "Camelopardalids 2014: visual data quicklook". `http://www.imo.net/live/cameleopardalids2014/` . (last accessed 2014 June 9).

Jenniskens P. (2006). *Meteor Showers and their Parent Comets*. Cambridge University Press, 790 pages.

Jenniskens P. (2008). "Mostly dormant comets and their disintegration into meteoroid sterams: A review". *Earth, Moon and Planets*, **102**, 505–520.

Jenniskens P., Gural P. S., Dynneson L., Grigsby B., Newman K. E., Borden M., Koop M., and Holman D. (2011). "CAMS: Cameras for Allsky Meteor Surveillance to validate minor meteor showers". *Icarus*, **216**, 40–61.

Jenniskens P. and Lyytinen E. (2014). "Possible new meteor shower from comet 209P/LINEAR". *Central Bureau Electronic Telegrams*, **3869**.

Murray I. S., Beech M., Taylor M. J., Jenniskens P., and Hawkes R. L. (2000). "Comparison of 1998 and 1999 Leonid light curve morphology and meteoroid structure". *Earth, Moon and Planets*, **82-83**, 351–367.

Rao J. (2014). "Strong new meteor shower to strike?". *Sky & Telescope*, pages 30–35. (May 2014).

Rudawska R. and Jenniskens P. (2014). "New meteor showers identified in the CAMS and SonotaCo meteoroid orbit surveys". In *Proc. Meteoroids 2013 Conf., Aug. 26-30, 2013*, A.M. University, Poznan, Poland. (in press).

Šegon D., Gural P., Ž. A., Skokić I., Korlević K., Vida D., and Novoselnik F. (2014). "New showers from parent body search across several video meteor databases". *WGN, Journal of the IMO*, **42**, 57–64.

Vaubaillon J. (2003). *Dynamics of meteoroids in the Solar System. Application to the prediction of meteoric showers in general and Leonids in particular*. PhD thesis, I.M.C.C.E., Observatoire de Paris, Paris, France.

Vaubaillon J. (2012). "The next big meteor shower". `http://www.imcce.fr/langues/en/ephemerides/phenomenes/meteor/DATABASE/209_LINEAR/2014/index.php?char=year&body=Earth&year=2014&shower=209_LINEAR` . (last accessed 2014 June 2).

Ye Q. and Wiegert P. A. (2014). "Will comet 209P/LINEAR generate the next meteor storm?". *MNRAS*, **437**, 3283–3287.

Handling Editor: Javor Kac